Journal of ELECTRICAL ENGINEERING, VOL 72(2021), NO1, 61–65

sciendo

PAPERS

Preparation and gas-sensing properties of very thin sputtered NiO films

Ivan Hotovy[1], Vlastimil Rehacek[1], Martin Kemeny[1], Peter Ondrejka[1], Ivan Kostic[2], Miroslav Mikolasek[1], Lothar Spiess[3]

We present results on very thin NiO films which are able to detect 3 ppm of acetone, toluene and n-butyl acetate in synthetic air and to operate at 300 °C. NiO films with 25 and 50 nm thicknesses were prepared by dc reactive magnetron sputtering on alumina substrates previously coated by Pt layers as heater and as interdigitated electrodes. Annealed NiO films are indexed to the (fcc) crystalline structure of NiO and their calculated grain sizes are in the range from 22 to 27 nm. Surface morphology of the examined samples was influenced by a rough and compact granular structure of alumina substrate. Nanoporous NiO film is formed by an agglomeration of small grains with different shapes while they are created on every alumina grain.

K e y w o r d s: NiO films, reactive magnetron sputtering, alumina substrate, gas sensors, acetone, toluene, n-butyl acetate

1 Introduction

Recently, we have noted great efforts by researchers to prepare new gas sensors as well as to integrate them into electronically controlled sensor arrays [1] seeking to improve their sensitivity and selectivity in different applications such as food quality control [2] environmental monitoring [3], non-invasive disease diagnosis [4] or detection of explosive and toxic gases for humans in dangerous concentrations [5]. Everywhere we see the need to identify small amounts of chemicals in the gaseous state. Over the last forty years of development, gas sensors based on various technologies, including thin films based on metal oxides, nanowires and nanotubes, have proven to have a considerable potential for detecting a wide range of chemical compounds.

Gas-sensing materials are usually manufactured using nanotechnologies which can offer a large area-to-volume ratio and thus provide increased sensor sensitivity. Physical (evaporation, sputtering) and chemical (chemical vapor deposition, hydrothermal methods) methods of thin film preparation are used to achieve optimal material characteristics [6]. In general, today's gas sensors are based on metal oxide semiconductors and require a high operating temperature (around 400 °C) for adequate sensitivity and response / recovery time.

Nickel oxide (NiO) is one of the versatile and technologically important p-type semiconducting materials with the band gap energy in the range from 3.6 to 4 eV [7]. It is an attractive material, well-known for its excellent optical and electrical properties. Recently, NiO has been investigated for applications such as catalyst in fuel cells [8], electrode materials for lithium ion batteries [9], electrochromic devices [10], supercapacitors [11], hole transporting layer in solar cells and also as a functional layer in metal oxide gas sensors due to its chemical stability and non-toxicity [12, 13].

In this study, NiO thin films deposited by dc reactive magnetron sputtering with 25 and 50 nm thicknesses were examined. Consequently, the sensor structures containing of NiO and Pt/Au were investigated with XRD and FESEM. Electrical responses of these sensors at operating temperature of 300 °C towards acetone, toluene and n-butyl acetate in concentrations less 5 ppm were measured and evaluated.

2 Experimental procedures

NiO films were deposited by dc reactive magnetron sputtering from a Ni target (4" in diameter, 99.99 % pure) in a mixture of oxygen and argon at room temperature. A sputtering power of 600 W was used. The relative partial pressure of oxygen in the reactive mixture O_2-Ar was 30 %. The total working sputtering gas pressure was kept at 0.5 Pa and adjusted by a piezoceramic valve. Details of these sputter-deposition conditions had been described elsewhere [14]. The film thicknesses measured by Talystep were about 25 and 50 nm for all examined samples. The NiO films were prepared on unheated alumina substrates previously coated and patterned by Pt layers

[1] Institute of Electronics and Photonics, Slovak University of Technology, Ilkovicova 3, 812 19 Bratislava, Slovakia, ivan.hotovy@stuba.sk
[2] Institute of Informatics, Slovak Academy of Sciences, Dubravska cesta 9, 845 07 Bratislava, Slovakia, [3] Department of Materials Technology, Technical University of Ilmenau, D-98684 Ilmenau, Germany

DOI:10.2478/jee-2021-0009, Print (till 2015) ISSN 1335-3632, On-line ISSN 1339-309X

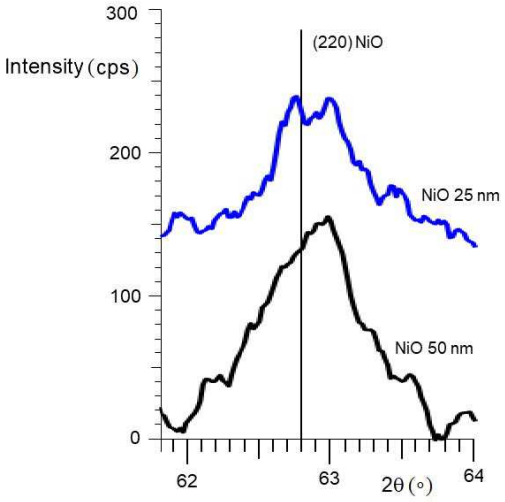

Fig. 1. NiO XRD patterns of NiO films with and nm thickness on alumina and ptalumina substrates

as microheaters and interdigitated electrodes for physical, structural and gas-sensing characterization. In order to stabilize the properties, all films were annealed in a furnace at 500 and 600 °C in dry air for 2 hours.

The crystal structure was identified with a Theta-Theta Diffractometer D5000 with a Goebel mirror in the grazing incidence geometry with CuKα radiation. The average crystalline grain size of Pt and NiO nanoparticles was estimated from the integral peak widths and positions using the Scherrer formula. The fabricated NiO sensor structures were observed in a field emission scanning electron microscope (FE SEM) Inspect F50 (*FEI*).

PTFE permeation tubes 120 mm long with outer diameter of 5 mm filled with various volatile organic compounds (acetone, toluene and n-butyl acetate were used for dispensing a small flow of permeate vapor through a polymeric membrane (wall). Since the permeation rate of the vapor is given not only by the permeability of the PTFE membrane itself but also by ambient temperature, the operating temperature of the tubes was held at 23 °C. To measure the permeation rate, the tubes were weighed over time intervals. The rate of weight loss is the permeation rate of the tube. In our case, the permeation rates were found 17 780 ng/min for acetone, 16 360 ng/min for toluene and 27 030 ng/min for n-butyl acetate.

A volatile liquid sealed inside the permeation tube was inserted in a 100 mL bottle gas washing (Drechsler). Dry synthetic air flowing over the bottle around the tube was mixed with the emitted vapor to form output vapor concentration. The output concentration in ppm was calculated according to equation

$$C_p = \frac{m_{\mathrm{VOC}}}{m_{\mathrm{air}}} \frac{M_{\mathrm{air}}}{M_{\mathrm{VOC}}} \times 10^6, \qquad (1)$$

where C_p is the primary concentration of outgoing volatile organic compounds from the bottle (ppm), $\mathrm{m_{VOC}}$ is the weight of emitted VOC per min (g), m_{air} is the weight of synthetic air flowing per min 8, M_{air} is the molar weight of synthetic air (g/mol) and M_{VOC} is the molar weight of VOC.

At an air flow rate of 100 mL/min through the bottle the output concentrations of vapors were calculated as 69 ppm for acetone, 40 ppm for toluene and 52 ppm for n-butyl acetate.

Since the air flow around the permeation tube can be used to achieve a concentration that is not sufficiently low at one-step dilution, a typical permeation system flow employs two-stage vapor dilution. At the secondary dilution step the primary mixture produced directly from the permeation tube is split off and diluted into an additional flow of air. In our case the output mixture from the bottle gas washing was additionally diluted 4 to 20 times. The final concentration of vapor VOCs was calculated according to equation

$$C = \frac{F_{\mathrm{dil}}}{F_{\mathrm{tot}}} C_p \,, \qquad (2)$$

where C is the final (secondary) concentration of VOC, F_{dil} is the air flow through the bottle (mL/min), F_{tot} is the total air flow (ml/min) and C_p is the primary concentration of VOC (ppm).

The response from NiO sensors towards vapor of VOCs was obtained by measuring the electrical resistance by an Agilent 34410 A multimeter recorded using a GPIB interface for communication with a computer by LabView platform. Programmable DC Power supply TP-3303 U (Twintex) was used as a power supply of the heater element. In all experiments the operation temperature of sensors was set to 300 °C. Using mass flow meters and controllers with a nominal flow of 25 and 1000 sccm, the mixed gas flows with the desired concentration were set. Sensors was placed in the measuring chamber with an inner volume of 31 cm^3. To keep the sensor operational temperature constant, the total flow rate of the mixture through the chamber was always kept at 100 mL/min. All chemicals (acetone, toluene and n-butyl acetate) were of analytical grade. Dry synthetic air was used as a carrier gas.

3 Experimental results and discussion

The diffraction peaks of the NiO and Pt thin films were joined on the basis of (fcc) NiO structure (PDF card No. 47-1049) and (fcc) Pt structure (PDF card No. 04-0802). In the case of Pt films, only the Pt (111) peak at 39.8° could be found. Polycrystalline nature with a texture in [111] direction was identified. Pt films with a thickness of about 200 nm always exhibited a columnar structure with a grain size of about 33 nm. The correct identification of NiO peaks in recorded diffractograms was negatively affected by the overlap of the NiO and Al_2O_3 peaks. The position of NiO (111) peak at 37.2° was close to the Al_2O_3 (110) peak at 37.8°. Another NiO (200) peak has the same position as Al_2O_3 (113) peak. Only the NiO (220) peak at $2\theta = 62.8°$ is not overlapped

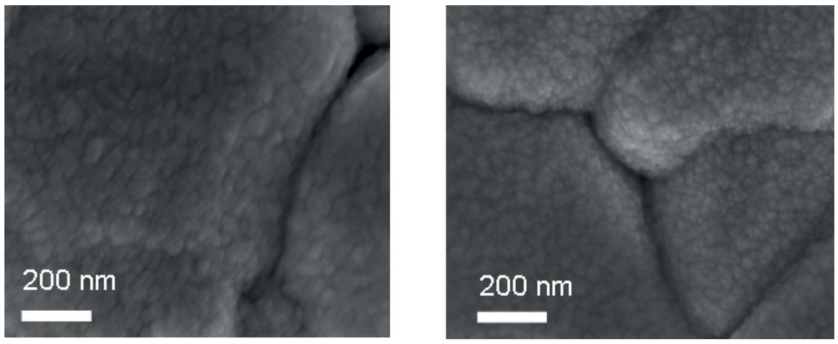

Fig. 2. FE SEM surface morphology of NiO films with different thickness on alumina and Pt/alumina substrates with: (a) – 25 nm, and (b) – 50 nm

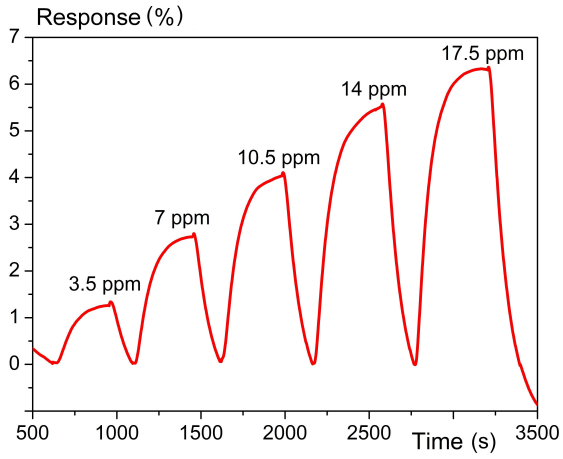

Fig. 3. Responses of NiO sensor with film thickness of 50 nm, annealed at temperature 600 °C for 2 hours in nitrogen atmosphere, to increasing the concentration of acetone in dry synthetic air at 300 °C

by any peaks belonging to Pt or Al_2O_3. Figure 1 shows that (220) peak positions of the NiO films deposited on alumina and Pt/alumina are close to the right position at 62.8° and both prepared NiO films can be indexed to the (fcc) crystalline structure of NiO. In Fig. 1 one can see that the recorded diffraction patterns for NiO films with 25 nm thicknesses exhibit lower intensities with a smaller amount of grains and these curves contain two or three separate peaks indicating perfect small grains. The average grain sizes of both investigated NiO films were in the range from 22 to 27 nm as calculated from the measured integral peak widths values for the (220) NiO plane.

Since the gas sensor structures were prepared on a rough alumina substrate, FE SEM observations were also done on the same samples to identify the effective morphology of sensor surfaces. It was observed from Fig. 2 that surface morphology of the examined samples was characterized by a rough and compact granular structure reflecting the alumina substrate surface. The nanoporous NiO film is formed by an agglomeration of small grains with different shapes while they are created on every alumina grain. NiO grows not only on top of the alumina grains but also on grain sides and along their grain boundaries and it is filling the space between Al_2O_3 grains. From Fig. 2 we can see that the average grain sizes in the lateral direction of the films prepared with 25 nm thicknesses are greater (10 nm) than for NiO films with 50 nm thicknesses (15 nm).

The gas sensing properties of NiO thin films with thickness of 25 and 50 nm annealed at 500 and 600° Cwere investigated upon exposure to various volatile organic compounds such as acetone, toluene and n-butyl acetate. The relative responses (R) of NiO sensors were determined by relationship

$$R = \frac{R_g - R_0}{R_0} \times 100, \tag{3}$$

where R_g is NiO resistance in tested vapor atmosphere and R_0 is NiO resistance in synthetic air atmosphere. The resistance changes of NiO films are caused by exchange of charges between the adsorbed gaseous species and the metal oxide surface. When NiO is placed in air at high temperature, oxygen molecules are adsorbed onto the NiO surface, which causes extraction of electrons from NiO and formation of different ionized oxygen species depending on temperature (O_2^-,O^-,O^{2-}) [15]. After exposure of NiO film to reducing gases (acetone, toluene and n-butyl acetate), electrons are injected into the material due to oxidation reaction between the reducing gas and oxygen anion species. Injection of electrons decreases the concentration of holes and thus increases NiO resistance as the NiO is a p-type semiconductor.

One of the factors affecting the sensitivity of metal oxide sensors is the grain size [16]. Since the sensitivity of metal oxides increases with the reduction in the grain size, the grain size decrease is one of effective strategies for enhancing the gas-sensing properties. Since an increase in the annealing temperature lead to an increment of surface roughness which is associated with the increase in grain size [17], we investigated the resistance of sensors with NiO films annealed at 500 and 600 °C in our experiments. The resistance of the NiO sensor prepared with 50 nm thickness and annealed at 500 °C under synthetic air atmosphere at operating temperature (300 °C) was found to be 12.8 kΩ, while for the same NiO sensor annealed

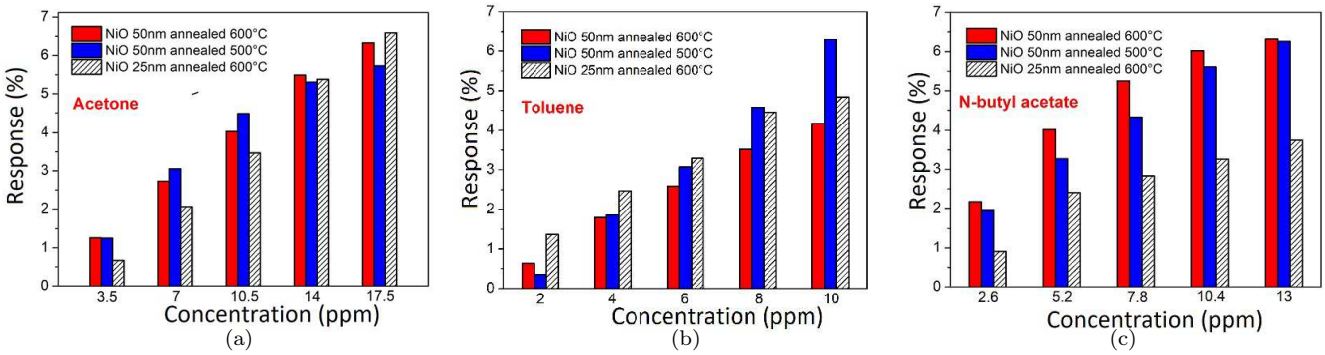

Fig. 4. Response in % of the various NiO sensors to increasing concentration of: (a) – acetone, (b) – toluene, and (c) – n-butyl acetate in dry synthetic air at operating temperature 300 °C depending on concentration in ppm

Table 1. Relative sensitivity values of various NiO sensors to different VOCs, R – correlation coefficient of linearity of the calibration curve, N/A* – response saturation

	Acetone		**Toluene**		**n-butyl acetate**	
Sample	Sensitivity (%/ppm)	R	Sensitivity (%/ppm)	R	Sensitivity (%/ppm)	R
50 nm 600 °C	037	0.996	0.44	0.996	N/A*	N/A*
50 nm 500 °C	N/A*	N/A*	0.73	0.998	0.42	0.994
25 nm 600 °C	0.43	0.998	0.48	0.989	0.20	0.991

Table 2. The effect of NiO film thickness and annealing temperature on response times for various VOCs

Sample	Acetone	Toluene	n-butyl acetate
	Response time in seconds		
50 nm 600 °C	188	166	206
50 nm 500 °C	98	130	124
25 nm 600 °C	92	89	76

at 600 °C as high as 88.5 kΩ. The better sensing performance of the sensor with lower resistance and most likely associated with the reduced grain size as confirmed in our experiments. In Fig. 3 typical responses are shown of NiO sensor prepared with 50 nm thickness at different concentration of acetone. The responses increased with increasing concentration of acetone (3.5 to 17.5 ppm) in the range from 0.7 to 6.6 % for all sensors.

Apparently, when comparing different NiO sensors (Fig. 4), no significant differences in responses were observed in the case of acetone. In the case of the toluene (2 to 10 ppm) and n-butyl acetate (2.6 to 13 ppm) the responses increased in the range from 0.4 to 6.3 % and 1.6 to 6.3 %, respectively, for all sensors. Only the responses to n-butyl acetate of NiO sensor prepared with 25 nm thickness and annealed at 600 °C were lower by roughly 30 to 40 % in comparison with other NiO sensors. In Table 1, NiO sensor sensitivities are compared with acetone, toluene and n-butyl acetate. These values were calculated from their calibration curves. In most cases, the relation between the responses of sensors and the concentrations of acetone, toluene and n-butyl acetate is close to linear in given ranges. Response saturation was observed in two cases. We found various dynamics of sensor responses (response/recovery time) in our experiments depending especially on the film thickness and the kind of volatile organic compound.

The response time is defined as the time required for the gas sensor to reach 90 % resistance change in the presence of the target gas, and the recovery time is defined as the time needed for the resistance of the gas sensor to return to 10 % of its original baseline value after the removal of the target gas. Response dynamics curve of NiO sensor prepared with 50 nm thickness and annealed at 500 °C towards 10.5 ppm acetone concentration is shown in Fig. 5. The response and recovery times for the same sensor are a little longer for 10 ppm toluene concentration (130/150 s) and for 10.4 ppm n-butyl acetate concentration (124/102 s) than for acetone. The effect of NiO film thickness on the response time was even more pronounced (Tab. 2).

The response times towards all examined organic vapors in the case of NiO sensor prepared with 25 nm thickness were 2, 1.9 and 2.7 times shorter than for NiO sensor prepared with 50 nm thickness. These recorded measurements confirmed that the sensors prepared with thinner gas sensing films are faster than those with higher thickness [14].

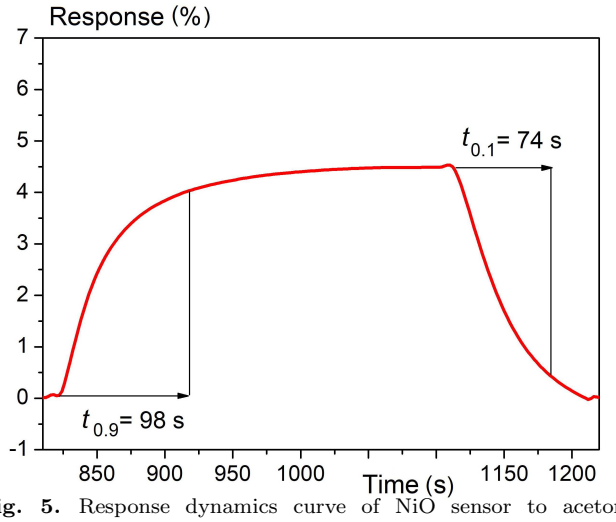

Fig. 5. Response dynamics curve of NiO sensor to acetone (10.5 ppm) at 300 °C

4 Conclusions

NiO thin films with 25 and 50 nm thicknesses were successfully fabricated by dc reactive magnetron sputtering. XRD investigations confirmed that both prepared NiO films are indexed to the (fcc) crystalline structure of NiO and the average grain sizes of both investigated NiO films were in the range from 22 to 27 nm. FE SEM observation revealed that surface morphology of the examined samples was characterized by a rough and compact granular structure reflecting the alumina substrate surface. Special attention was devoted to sensing properties towards acetone, toluene and n-butyl acetate with the concentrations less 5 ppm at the operation temperature of 300 °C. Our results demonstrate the potential of NiO thin films with 25 nm thicknesses to detect examined organic vapours shorter though with the same sensitivity compared to NiO sensors prepared with 50 nm.

Acknowledgements

The work was supported by the Scientific Grant Agency of the Ministry of Education of the Slovak Republic and of the Slovak Academy of Sciences, No. 1/0529/20 and 1/0789/21, by the Slovak Research and Development Agency under contract, No. APVV-17-0169, and German DAAD project 57243698.

References

[1] Zhesi Chen, Zhuo Chen, Zhilong Song, Y. Wenhao, and Zhiyong Fan, "Smart Gas Sensor Arrays Powered by Artificial Intelligence", *Journal of Semiconductors* 40 (2019), 111601.

[2] M. Penza and G. Cassano, "Chemometric Characterization of Italian Wines by Thin-Film Multisensors Array and Artificial Neural Networks", *Food Chem* 86 (2004), 283.

[3] L. Capelli, S. Sironi, and R. Del Rosso, "Electronic Noses for Environmental Monitoring Applications", *Sensors* 14 (2014), 19979.

[4] M. Hakim, Y. Y. Broza, O. Barash, *et al* , "Volatile Organic Compounds of Lung Cancer and Possible Biochemical Pathway", *Chem Rev* 112 (2012), 5949.

[5] J. Chen, Z. Chen, F. Boussaid, *et al* , "Ultra-Low-Power Smart Electronic Nose System Based on Three-Dimensional Tin Oxide Nanotube Arrays", *ACS Nano* 12 (2018), 6079.

[6] D. Punetha and S. K. Pandey "CO Gas Sensor Based on e-Beam Evaporated ZnO, MgZnO, and CdZnO Thin Films: a Comparative Study", *IEEE Sens J* 19 (2019), 2450.

[7] A. A. Al-Ghamdi, M. Sh. Abdel-wahab, A. A. Farghali, and P. M. Z. Hasan, "Structural, Optical and Photo-Catalytic Activity of Nanocrystalline NiO Thin Films", *Materials Res. Bulletin* 75 (2016), 71–77.

[8] R. S. Amin, R. M. Abdel Hameed, K. M. El-Khatib, M. Elsayed Youssef, and A. A. Elzatahry, "Pt-NiO/C Anode Electrocatalysts for Direct Methanol Fuel Cells", *Electroch. Acta* 59 (2012), 499–508.

[9] B. Varghese, M. V. Reddy, Z. Yanwu, S. Ch. Lit, T. Ch Hoong, G. V. S. Rao, B. V. R. Chowdari, A. T. S. Wee, T. Ch. Lim, and H. Ch. Sow, "Fabrication of NiO Nanowall Electrodes for High Performance Lithium Ion Battery", *Chem. Mater.* 20 (2008) 3360–3367.

[10] Y. Ren, W. K. Chim, L. Guo, H. Tanoto, J. Pan, and S. Y. Chiam, "The Coloration and Degradation Mechanisms of Electrochromic Nickel Oxide", *Solar Energy Mat. and Solar Cells* 116 (2013), 83–88.

[11] X. Zhang, W. Shi, J. Zhu, W. Zhao, J. Ma, S. Mhaisalkar, and T. L. Maria, "Synthesis of Porous NiO Nanocrystals with Controllable Surface Area and their Application as Supercapacitor Electrodes,", *Nano Res.* 3 (2010), 643–652.

[12] J. M. Choi, J. H. Byun, and S. S. Kim, "Influence of Grain Size on Gas-Sensing Properties of Chemiresistive p-Type NiO Nanofibers", *Sens. and Actuators* B 227 (2016), 149–156.

[13] Y. Lu, Y. H. Ma, S. Y. Ma, W. X. Jin, S. H. Yan, X. L. Xu, X. H. Jiang, T. T. Wang, H. M. Yang, H. Chen, and Z. Qiang, "Synthesis of Cactus-Like NiO Nanostructure and their Gas-Sensing Properties", *Materials Letters* 164 (2016), 48–51.

[14] I. Hotovy, L. Spiess, M. Predanocy, V. Rehacek, and J. Racko:, "Sputtered Nanocrystalline NiO Thin Films for Very Low Ethanol Detection", *Vacuum*, pp. 129–131, 2014.

[15] Y. Lu, Y. H. Ma, S. Y. Ma, W. X. Jin, S. H. Yan, X. L. Xu, and Q. Chen, "Curly Porous NiO Nanosheets with Enhanced Gas-Sensing Properties", *Materials Letters*, pp. 252–255, 2017.

[16] T. Lin, X. Lv, Z. Hu, A. Xu, and C. Feng, "Semiconductor Metal Oxides as Chemoresistive Sensors for Detecting Volatile Organic Compounds", *Sensors*, pp. 1–32, 2019.

[17] B. Comert, N. Akin, M. Donmez, S. Saglam, and S. Ozcelik, "Titanium Dioxide Thin Films as Methane Gas Sensors", *IEEE Sensors Journal*, pp. 8890–8896, 2016.

Received 20 January 2021